Symmetry Breaking and Electrostatic Attraction between Two Identical Surfaces

F. Plouraboué[a], H.-C. Chang[a]

[a]*IMFT UMR CNRS-INPT-UPS No.*5502 *Av. du Professeur Camille Soula,* 31400 *Toulouse, France*
[b]*Center for Micro-fluidics and Medical Diagnostics and Department of Chemical and Biomolecular Engineering, University of Notre Dame, Notre Dame, IN 46556, USA*

Abstract

By allowing the surface charge of one surface to affect the adsorption equilibrium of the other, we establish the existence of a long-range attractive interaction between two identical surfaces in an electrolyte containing polyvalent counter ions with a mean-field Poisson-Boltzmann approach. A Stern electrostatic condition from linearization of the mass-action adsorption isotherm is used to capture how polyvalent ion condensation affects and reverses the surface charge. We furthermore establish a direct mapping between this Stern layer conditions and previously derived modified Mean-field formulations associated with correlated fluctuations theory. For a sufficiently potential-sensitive isotherm, anti-symmetric charge inversion can occur to produce an attractive force that increases with decreasing ionic strengths. Analyses of a mass-action isotherm produce force-separation relations, including an exponential far-field force decay distinct but consistent with previously proposed correlated fluctuation theories, and in quantitative agreement with experimental data.

Keywords: Stern layer, correlated fluctuations theory, modified Mean-field theory, Poisson-Boltzmann problem, attraction between identical surfaces

1. Introduction

Recent atomic force microscopy studies have shown that, in the presence of a polyvalent counterion, two similarly charged or identical surfaces can develop an attractive force at a distance comparable to the Debye screening length λ [1, 2]. This observation is most likely related to earlier reports on attraction between identical colloids in an electrolyte, although the role of poly-valency is not as well established for colloids [3, 4]. It is also related to the condensation of likecharged molecules like DNAs [5]. It has been rigorously shown that, for two identical spheres with constant potential [6] the inter-particle interaction is necessarily repulsive according to the classical Poisson-Boltzmann (PB) mean-field theory [6]. For this reason, theories for like-charge attraction phenomena have sought mechanisms beyond the classical mean-field description to include spatial correlation of charge fluctuations [7, 8, 9, 10].

Such fluctuation theories suggest cross-surface spatial correlation either between fluctuations of the condensed counter-ions in the Stern layer [11] or between surface Wigner crystalss [12] that are formed by the same ions. However, when the two surfaces are separated by a distance larger than the Bjerrum length, thermal noise is expected to disrupt the fluctuation correlation of condensed ions on the two surfaces. Also strong concentration gradients develop within the Debye layer which may invalidate the assumptions of many correlated fluctuation theories.

Although AFM measurements of [1] and recent MD simulation of DNA condensation does not show surface ion ordering [13], correlated fluctuations should nevertheless play a role during ion

condensation onto charged surfaces [14] especially for polyvalent electrolytes counterions [2].

However, connecting the fluctuations at a Bjerrum length separation from the surface to longer range attraction over the Debye length is still unclear. More specifically, theories for correlated layers charges between two parallel plates separated by a distance $2h$ much larger than the Debye length λ, give rises to an effective "long-range" dipolar attractive pressure, $p \sim 1/(2h)^3$ [15], an almost dipolar one $p \sim \ln[2h/\lambda]/(2h)^3$ [7, 9], or a modified exponential attraction $p \sim \exp^{-4h/\lambda}/2h$ [16, 17]–also found in colloids interactions [18]– whereas the classical DLVO theory only predicts a repulsive exponential behaviour $p \sim \exp^{-2h/\lambda}$.

In this paper, we lump short-range correlated fluctuation effects into a linear empirical isotherm for polyvalent counter-ion condensation that captures charge inversion.

We then show that this linear Stern isotherm condition can induce asymmetric charge inversion and PB ion distributions due to nonlinear field screening/enhancement of the space charge and field-enhanced condensation effects on the two surfaces.

The paper is organized as follows. We describe in section 2.1) the classical Stern-layer boundary condition in its usual formulation. In section 3 we first discuss the linear Debye-Hückel (D-H) approximation with Stern layers in order to find the bifurcation points for the non-linear Poisson-Boltzmann solutions which are further analyzed analytically in 3.2. Section 4 is devoted to the numerical computation of the main caracteristics of these solutions such as the surface potential and the interaction force with Stern layer parameters and dimensionless gap. Finally our findings are compared with available experimental data in section 6. We first show in 6.1 that adsorption isotherm linearization leads to Stern layer boundary conditions. We then compare long-range force behaviour predicted by our theory with experimantal measurements in section 6.

2. Modified Mean-field description

2.1. Stern layer boundary condition

Assuming rapid polyvalent counterion condensation kinetics, the isotherm stipulates that the surface charge density σ on a surface is a function of the Stern layer potential ϕ and the bulk electrolyte concentrations.

The potential ϕ represents the electrical potential difference between a bulk charge with a zero reference potential and that of a condensed/ adsorbed polyvalent counterion on the surface in the presence of an electric field. The condensed state then represents a free energy minimum, where the free energy includes the above electric potential, the entropy loss due to condensation and the interaction potential among the counter-ions and the surface. All three quantities are complex functions of the condensed polyvalent counterion condensation. As such, the free energy minimum represents a complex isotherm relationship for the equilibrium condensed counter-ion concentration as a nonlinear function of the potential difference and the bulk concentration. The surface charge σ is then the sum of the orignal field-free surface charge and those of the condensed counterions. A typical calculation of the nonlinear isotherm for the net charge density has been done by Zohar *et al.* [1] and is shown in Section 6. It contains various equilibrium association and dissociation constants for the counterion condensation reaction— the mutual interaction of the condensed counterions and the surface-counterion interaction . The net surface charge σ vanishes at a particular isoelectric potential ϕ_0 where the field-induced condensation has reversed the surface charge.

At a given bulk electrolyte concentration, σ is a nonlinear function of ϕ . One can, however, linearize this expression at the isoelectric potential ϕ_0 to obtain a σ that is proportional to $\phi - \phi_0$. Using a Gauss volume that confines the condensed charges within the Stern layer and assuming there is no field on the solid side, a simple integration of the Poisson equation indicates that this net charge σ is proportional to the normal surface electric field just outside the condensed ions $\partial_z \phi$. If we now assign this normal field outside the

condensed Stern layer as the boundary condition for the Poisson equation beyond it, we obtain

$$\partial_z \phi = \pm K[\phi - \phi_0], \qquad (1)$$

where the inverse Stern slip length K is determined by various association/dissociation equilibrium constants of participating ions and the iso-electric potential ϕ_0 represents the compensate Zeta potential on the true surface due to polyvalent ion condensation.

The Stern slip length can take on either sign, depending on the charge of the polyvalent counterion, the monovalent counterions, the uncompensated surface and the complex interaction (chemistry) among them. In Stern's classical context, this boundary condition represents the field across the Stern layer with the condensed counterion and ϕ_0 is the potential just outside the Stern layer. The inverse Stern slip length K is then related to the thickness of the condensed layer and the surface density of the condensed counterions, with different signs accounting for the charge of the polyvalent counterion. Our analysis is for two planar surfaces although extension to spheres can be carried out with the classical Derjaguin formulation. We scale the normal coordinate z by h, the half-separation between the two surfaces and the potentials ϕ and ϕ_0 by $RT/ZF = k_B T/Ze$, the thermal energy per valency measured in electric potential, where R is the ideal gas constant, T the temperature, Z the monovalent counterions valency, F the Faraday constant, k_B the Boltzmann constant, e the electron charge. From this we obtain an expression identical to (1) but with dimensionless variables

$$\partial_z \phi(\pm 1) = \pm \mu \sqrt{\beta}[\phi(\pm 1) - \phi_0], \qquad (2)$$

where we define the dimensionless separation squared as $\beta = (h/\lambda)^2$, so that the dimensionless K in (1), scaled by the separation h has been decomposed in $K = -\mu\sqrt{\beta}$ such that μ is only a function of the electrolyte composition. The magnitude of μ measures the effect of the Stern layer potential (and external field) on the adsorption isotherm.

With the same scaling, the PB equation for symmetric electrolytes is

$$\partial_z^2 \phi = \beta \sinh \phi, \qquad (3)$$

which will be solved with (2) for $z = \pm 1$. We note that, (2) and (3) are symmetric to the transformation $\mu \to -\mu$ and $z \to -z$. Hence the sign of μ is arbitrary and will be taken to be negative, so that μ is a positive constant. For any value of ϕ_0, symmetric solutions always exit, but anti-symmetric solutions are only permitted for $\phi_0 = 0$.

In section 6.1 we derive the Stern layer parameters from the adsorption isotherm linearization parameters, which are more easy to relate to some given experimental condition. One can also find in [19] the derivation of Stern layer parameters from previous derivation related to the correlated fluctuation theory of Lau *et al.* [9, 10].

3. Solution to the PB problem with Stern layers

In this section we solve the PB problem associated with boundary conditions (2). We first investigate the linear approximation associated with the Debye-Hückel (D-H) approximation, and then explore the features of the solution to the full nonlinear problem.

3.1. D-H approximation

Even though the linearized version of (3) does not produce any interaction, we still use the linear Debye-Hückel (D-H) approximation to determine the bifurcation of non-trivial solutions. Two linearized solutions exist, one symmetric (denoted with a capital S) and one non-symmetric (denoted with NS) with respect to reflection across midplane,

$$\phi^S = \cosh(\sqrt{\beta}z), \qquad (4)$$

$$\phi^{NS} = \frac{e^{\sqrt{\beta}z}}{2} + \left(\frac{2\mu\phi_0}{\sqrt{\mu^2 - 1}} - 1\right)\frac{e^{-\sqrt{\beta}z}}{2}. \qquad (5)$$

The coefficients of these eigenfunctions cannot be specified for the homogenized versions of (2) and (3). However, the corresponding linear operator becomes singular at

$$\beta_c^S = \left(\ln\left[\frac{-\mu\phi_0 + \sqrt{\mu^2\phi_0^2 + (1-\mu^2)}}{(1-\mu)}\right]\right)^2, (6)$$

3

$$\beta_c^{NS} = \left(\frac{1}{2} \ln \frac{\mu + 1}{\mu - 1} \right)^2, \tag{7}$$

where non-trivial solutions can bifurcate from the trivial solution 0. We note that for non-symmetric solutions (anti-symmetric in the case $\phi_0 = 0$), only $|\mu| > 1$ is possible, or, more precisely, $\mu > 1$ since we are restricted to positive μ values.

3.2. Solution to Poisson-Boltzmann problem

Equation (3) is integrable and its first integral is

$$\frac{1}{2} \left(\partial_z \phi \right)^2 = \beta \cosh \phi + d, \tag{8}$$

where d is a constant which depends on μ, β, ϕ_0 and the surface potential. Evaluating this integral at $z = \pm 1$ as a reference point, one obtains

$$d' = \frac{d}{\beta} = \frac{1}{2} [\mu(\phi(\pm 1) - \phi_0)]^2 - \cosh \phi(\pm 1). \tag{9}$$

This parameter can be related to the force between the two surfaces. Using Green's theorem and including the osmotic pressure from the bulk solution at the infinities behind the two surfaces [6], the pressure (force per unit area) between the two surfaces is can be derived,

$$
\begin{aligned}
p &= \left(-\frac{1}{2\beta} (\partial_z \phi)^2 + \cosh \phi - 1 \right) \\
p &= -d' - 1 \\
p &= -\frac{[\mu(\phi(1) - \phi_0)]^2}{2} + \cosh \phi(1) - 1
\end{aligned} \tag{10}
$$

where the dimensionless pressure p has been normalized by the Debye Maxwell stress $\epsilon(RT/zF\lambda)^2$ for convenience to remove the dependence on separation. It is independent of z and hence its value at $z = 1$ is evaluated by using (9). Looking at the last expression of (10) it is obvious that the osmotic pressure difference in the second term is always repulsive and the Maxwell pressure in the first term is always attractive, leading apparently to possible attractive or repulsive forces depending on $\phi(1)$ or d'. Nevertheless it can be easily shown by evaluating the pressure at $z = 0$ for the case of $\phi(0) = 0$ associated with anti-symmetric solution for $\phi_0 = 0$, in the first expression of (10) that the only remaining term at the origin is
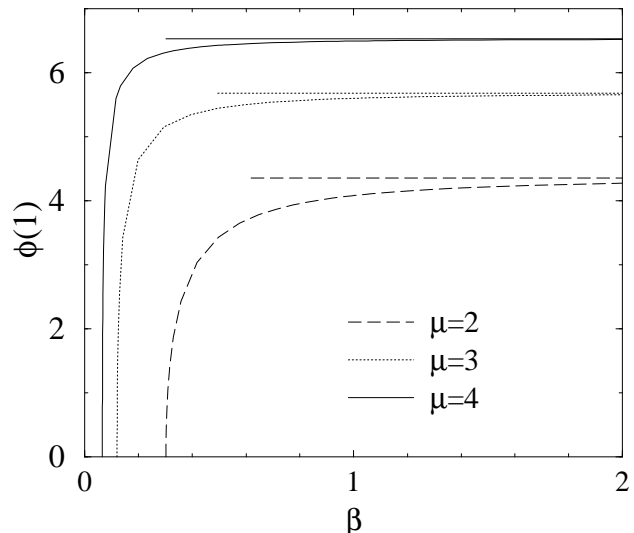

Figure 1: Surface potential of asymmetric solution $\phi(1)$ at $z = 1$ versus dimensionless gap β for $\phi_0 = 0$. The dotted lines display the value $\phi^\infty(1)$ obtained from solving (16).

the attractive Maxwell pressure. Hence all anti-symmetric solutions near the isoelectric point are attractive. Furthermore, some observations can be made at the (D-H) limit of small $\phi(1)$. Expansion of the osmotic pressure term shows that attractive interaction is only possible for $\mu > 1$, which is consistent with the previous observation that anti-symmetric solutions are only possible for this parameter range.

The required solution can be simplified by the Boltzmann transformation

$$\psi = \exp^{-\frac{\phi}{2}}, \tag{11}$$

such that the first integral (8) is transformed to

$$
\begin{aligned}
\partial_z \psi &= \pm \frac{\sqrt{\beta}}{2} \sqrt{\psi^4 + 2\frac{d}{\beta}\psi^2 + 1} \\
\partial_z \psi &= \pm \frac{\sqrt{\beta}}{2} \sqrt{(\psi^2 - \alpha_-)(\psi^2 - \alpha_+)},
\end{aligned} \tag{12}
$$

where,

$$\alpha_\pm = -d' \pm \sqrt{d'^2 - 1}, \tag{13}$$

are complex conjugate roots. Integrating (12) one more time leads to

$$\pm \frac{\sqrt{\beta}z}{2} + c = -\sqrt{\alpha_-} F_1 \left(\psi \sqrt{\alpha_+}, \alpha_- \right), \tag{14}$$

4

where F_1 is the elliptic integral of the first kind. Evaluating (14) at $z = \pm 1$ gives a transcendental equation for the potential values at boundaries:

$$\sqrt{\beta} = -\sqrt{\alpha_-}\left[F_1\left(\psi(1)\sqrt{\alpha_+}, \alpha_-\right)\right. \\ \left. -F_1\left(\psi(-1)\sqrt{\alpha_+}, \alpha_-\right), \right. \quad (15)$$

which complements Eq.(9), (11) and Eq.(13) to produce a set of two transcendental equations for $\phi(\pm 1)$ that can only be solved numerically.

4. Numerical computation and results

Albeit $\alpha_\pm$ is complex, and thus elliptic integral of the first kind with complex variables are needed for this computation, the solutions are always real and are symmetric with respect to $\alpha_\pm$. We use a Newton–Picard method for the evaluation of the unknown surface field $\phi(1)$, and continuously vary the parameters β and μ with a continuation method. The pitchfork bifurcation of these antisymmetric solutions from the bifurcation point $\beta_c^{NS}(\mu)$ of (7) is shown in Fig. 1 for different values of μ. It is evident that $\phi(1)$ first rises beyond a critical dimensionless separation β_c^{NS} and very rapidly reaches a constant asymptotic value $\phi^\infty(\mu)$ which depends only on μ at large separations, i.e for large value of β. This asymptotic value is concomitantly reached when d' tends to -1, and $\alpha_\pm$ to 1 so that the arguments of the elliptic function in (14) reaches 1 where it display a unique logarithmic singularity to compensate for large value of β on the left-hand-side. In this limit, one can evaluate the potential $\phi^\infty(\mu)$ from solving the simple transcendental equation

$$[\mu(\phi^\infty - \phi_0)]^2 = 2(\cosh\phi^\infty - 1) \quad (16)$$

found from (9). This values is illustrated for $\phi_0 = 0$ in Fig. 1.

Other computations in the $\phi_0 - \mu$ plane can also be found in [19].

5. Attractive behaviour

From knowing the surface potential one can easily deduce from (10) the negative pressure associated with iso-electric point anti-symmetric solutions. This negative pressure is plotted in Fig.
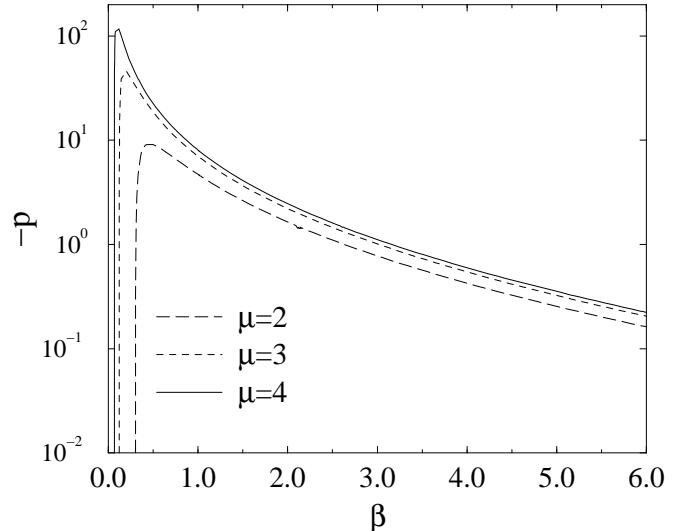

Figure 2: Semi-logarithmic plot of the attractive force per unit surface p versus the square of the dimensionless half-gap β for different values of parameter μ and $\phi_0 = 0$.

2a. The sharp maximum of the pressure in Fig. 2 is at the same value of β_m for which the potential gradient at the origin reaches a maximum (which is obvious from examining the first relation (10)). It is interesting to observe that the maximum force depends exponentially on the μ parameter. It might be a very sensitive way of estimating the parameter μ. When moving further apart from the iso-electric point, one find that the attractive region exists only for a finite range of separation β which are larger than β_c^{NS}, as illustrated in Fig. 2b. Repulsion due to native charges responsible for the effective Zeta potential ϕ_0 reduces the attractive region until it disappears completely beyond a critical ϕ_0. The repulsion also gives rise to a shallow maximum, a threshold pressure, as seen in Fig. 2b.

As previously discussed, the large gap limit is interesting to consider and compare to the usual (D-H) limit for the force. In this limit, the parameter d' approaches value -1, which corresponds to the vicinity of the logarithmic singularity of the elliptic function. Using known asymptotic behavior of the elliptic function near this singularity, it is possible to evaluate analytically the force distribution using, (9), (10) and (14)

$$\text{for } \beta \gg 1 \quad p \sim -\exp^{-2\sqrt{\beta}} \sim -\exp^{-2\frac{h}{\lambda}} \quad (17)$$

5

We compare this asymptotic behavior against the numerical results in the inset of Fig. (2)a and show very good agreement for β values as small as 3. It is interesting to note that the slope of the curves is independent of μ, as predicted by (17).

6. Comparison with experiments

6.1. Derivation of Stern layer parameters from adsorption isotherm linearization

In this section we use the "classical" derivation for Stern layer parameters from adsorption isotherm linearization. We evaluate the μ and ϕ_0 parameters from the isotherm proposed in Zohar et al. [1] for the net surface charge density σ at different trivalent Cobalt hexamine concentrations. The isotherm is derived from simple mass-action kinetics whose parameters are either measured or estimated with simple arguments, shown to be inconsistent with phase-locked Wigner crystals

$$\sigma(\phi) = -n_{Si}e\frac{1 - K_1[\text{Co}]\exp^{-3\phi}}{1 + K_2[\text{Co}]\exp^{-3\phi}} \quad (18)$$

Where e is the electron charge, [Co] the Cobalt hexamine concentration, ϕ the dimensionless potential rescaled by RT/ZF, $K_1 = 10^4 M^{-1}$ and $K_2 = 5\,10^3 M^{-1}$ are two empirical constants related to the association and dissociation rates and n_{Si} is the density of ionizable silanol groups which is estimated to range between $n_{Si} \simeq 0.3\text{-}1\,\text{nm}^{-2}$. The surface electro-neutral condition $\sigma(\phi_0) = 0$ leads to a simple dependence between the compensated Zeta potential ϕ_0 at a particular counterion concentration

$$\phi_0 = \frac{\ln(K_1[\text{Co}])}{3}, \quad (19)$$

A first order Taylor expansion of (18) about this reference point leads to

$$\sigma(\phi) \simeq -2n_{Si}e(\phi - \phi_0) \quad (20)$$

The application of Gauss theorem at the surface location $z = 1$, for dimensionless potential rescaled by $RT/ZF = k_BT/Ze$ leads to

$$\partial_z\phi = -2\frac{Ze}{k_BT}\frac{n_{Si}eh}{\epsilon}(\phi - \phi_0) \quad (21)$$

From identifying the constant of this affine relation to the Stern condition (2) with $K = -\mu h/\lambda$ one finds

$$\mu = 2Z\ell_B\lambda n_{Si} \quad (22)$$

where, again, $\ell_B \equiv e^2/\epsilon k_BT$ is the Bjerrum length. It is then interesting to compare (22) with the previous expression derived from the theoretical two-fluid model of Lau et al. in [19]. The condensed ion density n_C in the theoretical derivation of constant μ proposed in [19] is replaced by the density of ionizable silanol groups n_{Si} in its empirical counterpart given in (22). Since they both represent the surface density of negative charges at the solid surface, this give a consistent picture of how the parameter μ is related to physical constants. Moreover, since n_C is a theoretical prediction of the surface charge density (which could be related to other physical parameters from charge condensation mecanism as explained in [20]) where n_{Si} is related to an experimental estimate of the same quantity, both expression are fully consistent with either a theoretically or experimentally derivated expression for μ. Finally, it is hence surprising that such different approaches for estimating parameter μ only quantitatively differ by a prefactor which is $2Z$ in one case and πZ^2 in the other case. The different dependence with the valency Z could be attributed to the fact that in the experimental case, the negative charges associated with silanol groups are generally considered as monovalent.

The range of possible experimental value for n_{Si}, leads to $\mu = 1.32\text{-}4.4$. Furthermore relation (19) produces negative values of ϕ_0 for these experimental condition. However, as the problem is invariant with the transformation $(z, \phi, \phi_0) \rightarrow (-z, -\phi, -\phi_0)$, our results obtained for positive ϕ_0 also applies for negative ones.

6.2. Comparison with experimental force

The configuration which is analyzed in this paper is associated with two parallel identical surfaces. Nevertheless, the available experimental fine measurements of the force between similar surfaces in an electrolyte have all been performed with Atomic Force Microscopy (AFM) [4, 2, 1].
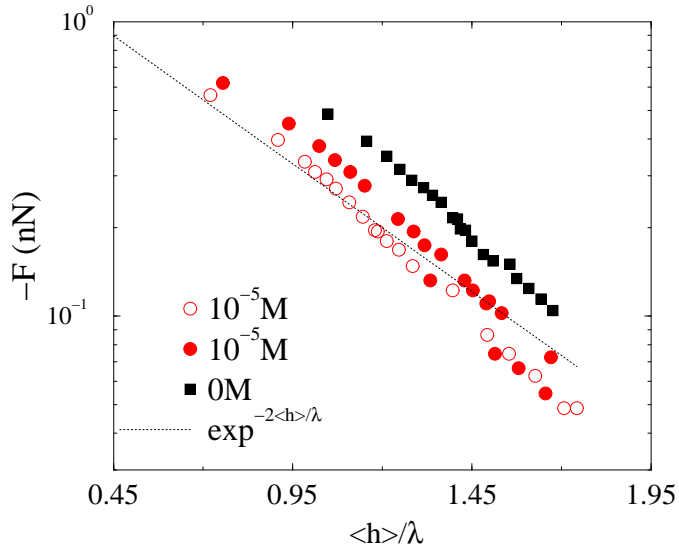
Figure 3: Test of the long-range scaling (17) for the data collected from Fig. 1b of [2] associated with different concentrations of $LaCl_3$ salt with an adjusted equivalent half-mean separation $\langle h \rangle$. The experimental Debye-length values λ are those given in [2].

Those measures are associated with a sphere/plane configurations. Nevertheless some features of the predicted attraction force between two parallel planes can be possibly extended when the ratio between the AFM tip distance to the wall to its radius of curvature is small [17, 4, 19].

As mentionned earlier in section 1, different theoretical predictions have been proposed for the long-range behaviour of the possibly attractive force of an electrolyte confined between two identical walls distant by a half-gap h. Nevertheless, few of these predictions have been sucessfully compared with experiments but the modified exponential attraction

$$p \sim \frac{\exp^{-4h/\lambda}}{2h} \qquad (23)$$

has been proposed in [16, 17] and experimentally tested in [4].

Nevertheless, there might be some caution for a definite answer to this question since the proposed modifyed exponential behavior very slightly differ from a pure exponential behaviour more recently reported in [1, 2]. Nevertheless, to our knowledge, the possibility of non exponential, algebraic far field decay proposed in [15, 7, 9] has

never received any convincing experimental evidence. Futhermore, since most of the experimental evidence for a modified exponential attraction is tested on semi-logarithmic coordinates in [4], and given the fact that experimental observation are also relatively noisy, it is hard to draw a definite conclusion on a possible logarithmic corrections to a mere linear trend of $\ln p$ versus h in (23). Moreover, most of the correction to the linear behaviour in figure 2 of [4] is concentrated in the close region where it is higly possible that the far-field asymptotic regime break-down.

On the contrary, our exponential decay of long-range attraction (17) is consistent with various experimental observations [1, 2]. To the best of our knowledge, our approach is the only one which predicts a pure exponential asymptote for the attractive force found in [2]. We verify this statement by analysing the slope of the exponential decay of the experimental measurements of [2].

Using the equivalent gap $\langle h \rangle$ deduced from the observed h_m associated with $LaCl_3$ salt analyzed in [2], we plot in figure 3 the experimental pressure as well as our theoretical prediction $p \sim \exp^{-2\langle h \rangle / \lambda}$. The resulting slope in log-linear scale very satisfactorily compared with our theoretical prediction as previously stated in relation (1) of Besteman et al.'s paper [2] independently of parameter μ. Hence not only our prediction quantitatively agree with a pure exponential decay, but the obserbed slope in semi-logarithmic representation also leads to satisfactory comparison with experimental data.

7. Conclusion

We have shown that it is possible to obtain an attractive anti-symmetric solution for the potential distribution of an electrolyte between two identical surfaces by taking into account the coupling between surface charge across the double layer due to the effect of each field on the condensation of polyvalent counterions on the other, as captured by a simple linear Stern condition derived from common isotherms obeying mass-action kinetics. We show analytically that asymmetric charge inversion and attraction are pos-

sible and we produce numerical results that are qualitatively and quantitatively consistent with experimental data. Our results reconcile correlated fluctuation theory based attraction, Stern layer models and available experimental observations. We are grateful for inputs from Y.E. Zhu, X. Cheng, C. Beaume and S. Basuray, and fruitful discussions with Pr. E. Trizac.

References

[1] Zohar O., Leizerson I., Sivan U., Short range attraction between two similarly charged silica surfaces, Phys. Rev. Lett. 96 (177802).

[2] Besteman K., Zevenbergen M. A. G., Heering H. A., Lemay S. G. , Direct observation of charge inversion by multivalent ions as a universal electrostatic phenomenon, Phys. Rev. Lett. 93 (17) (2004) 170802–06.

[3] Claesson P. M. , Christenson H. K. , Very long range attractive forces between uncharged hydrocarbon and fluorocarbon surfaces in water, J. Chem. Phys. 92 (1988) 1650–1655.

[4] Kékicheff P., Spalla O., Long-range electrostatic attraction between similar, charge-neutral walls, Phys. Rev. Lett. 75 (1995) 1851–1854.

[5] Gelbart W. M. , Bruinsma R., Pincus P., Parsegian V., DNA inspired electrostatic, Physics Today (2000) 38.

[6] Neu J. C. , Wall mediated forces between like-charged bodies in an electrolyte, Phys. Rev. Lett. 82 (5) (1999) 1072 – 1074.

[7] Lukatsky D. B. , Safran S. A. , Pressure correlated layer-charge and couterion fluctuations in charged thin films, Phys. Rev. E 60 (5) (1999) 5848–57.

[8] Netz R. R. , Orland H., Beyond poisson-boltzmann : fluctuations effect and correlation functions, Eur. Phys. J. E. 1 (2000) 203–214.

[9] Lau A. W. C. , Pincus P. , Counterions condensation and fluctuations-induced attraction, Phys. Rev. E 66 (041501) (2002) 041501.

[10] Lau A. W. C., Fluctuations and correlation effects in a charged surface immersed in an electrolyte solution, Phys. Rev. E 77 (011502) (2008) 011502.

[11] Oosawa F., Interaction between parallel rodlike macroions, Biopolymers 6 (11) (1968) 1633–1647.

[12] Gronbech-Jensen N., Mashl R. J. , Bruinsma R. F., Gelbart W. M., Counterion-induced attraction between rigid polyelectrolytes, Phys. Rev. Lett. 78 (1997) 2477 – 2480.

[13] Dai L., Mu Y., Nordenskiold L., J. R. C. van der Maarel, Molecular dynamics simulation of multivalent-ion mediated attraction between dna molecules, Phys. Rev. Lett. 100 (2008) 118301.

[14] Grosberg A. Y. , Nguyen T. T. , Shklovskii B. I., Colloquium : The physics of charge inversion in chemical and biological systems, Rev. Mod. Phys. 74 (2002) 329–345.

[15] Attard P., Kjellander R., Mitchell D. J., Electrostatic fluctutations interactions between neutral surfaces with adsorbed mobile ions or dipoles, J. Chem. Phys. 89 (3) (1988) 1664–1680.

[16] Podgornik R., Electrostatic correlation forces between surfaces with surface specific ionic interactions, J. Chem. Phys. 91 (1989) 5840–5849.

[17] Spalla O. , Belloni L., Long range electrostatic attraction between neutral surfaces, Phys. Rev. Lett. 74 (13) (1995) 2515–2518.

[18] Belloni L., Spalla O., Attraction of electrostatic origin between colloids, J. Chem. Phys. 107 (2) (1997) 465–480.

[19] Plouraboué F., Chang H.-C., Symmetry breaking and electrostatic attraction between two identical surfaces, Phys. Rev. E, 79, (041404).

[20] Lau A. W. C. , Lukatsky D. B., Pincus P., Safran S. A., Counterions condensation and fluctuations-induced attraction, Phys. Rev. E 65 (051502).